Light Curves of a Type II Supernova AT2023hpb

Department of Physics, University of California, Santa Barbara, CA

June 13, 2023

Abstract

We analyze the light curves of a recently discovered supernova, AT2023hpb, with the method of photometry. After modeling its light curves in each filter and comparing them with the theoretical light curves of different types of supernovae, we conclude that the objective supernova should be classified as Type II.

1 Introduction

1.1 Light Curves of Supernovae

In this observational experiment, we analyzed the light curves of a recently discovered supernova, AT2023hpb, with the method of photometry. A supernova is a luminous explosion of a star in which sudden change of light magnitude can be observed through time. A light curve of a supernova is a graph of the supernova's apparent magnitude as a function of time, typically measured in a particular frequency interval or band. Generally speaking, supernovae are classified into two categories based on the presence of hydrogen lines in their spectrum: If hydrogen lines are measured, then the supernova is classified as Type II; otherwise it is Type I. As a result, Type I supernovae always have light curves with a sharp maximum and a rapid decline of luminosity, while Type II supernovae always have light curves with less sharp maximum and less rapid decline of luminosity (As convention, higher apparent magnitude indicates lower luminosity of the star). The two types of supernova can be classified into sub-types according to the presence of other elements and the shape of light curve [10]. For example, Type I supernovae can be further classified by Type 1a which presents a singly ionised silicon (Si II) line at 615.0 nm near peak light, and Type 1b/c which doesn't have this spectrum line. Also, Type II supernovae can be classified Type II-P, which reaches a "plateau" in its light curve, and Type II-L, which displays a "linear" decrease in its light curve, which is shown in Fig. 1 [2].

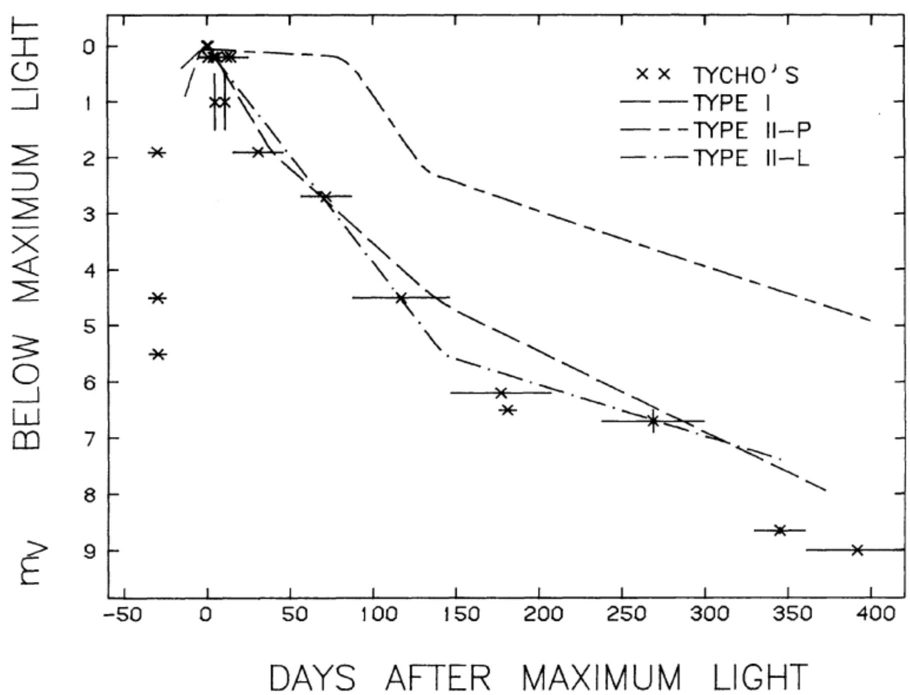

Figure 1: Comparison of the light curves of Tycho's supernova with the mean visual light curves of Type I, II-P, and II-L supernovae. Horizontal lines through the data points indicate the time interval to which the magnitude estimate applies, and vertical lines refer to an estimated magnitude range. [2]

1.2 Formation of Type II Supernovae

Different types of supernovae are corresponding to different astrophysical explanation of the formation of those supernovae. Studies show that most supernovae are formed either by runaway nuclear fusion triggered in a white dwarf or by sudden gravitational collapse of a massive star's core. The first mechanism of thermal runaway corresponds to Type Ia supernovae, and the second mechanism of core collapse corresponds to all other types of supernovae. With those scientific models, we are able to predict the future of the supernovae by identifying the change of their apparent magnitude.

Specifically, a Type II supernova results from the rapid collapse of a massive star. A star must have at least eight times, but no more than 40 to 50 times, the mass of the Sun to undergo this type of explosion [3]. Unlike the Sun, massive stars possess the mass needed to fuse elements that have an atomic mass greater than hydrogen and helium. The star fuses increasingly higher mass elements, starting with hydrogen and then helium, progressing up through the periodic table until a core of iron and nickel is produced. Due to the lack of energy, the core contracts due to gravity until the overlying weight of the star can be supported largely by electron degeneracy pressure.

When the compacted mass of the inert core exceeds 1.4 times of the mass of the sun, electron degeneracy is no longer sufficient to counter the gravitational compression. A implosion of the core takes place within seconds. Without the support of the imploded inner core, the outer core collapses inwards under gravity and reaches a velocity of up to 23% of the speed of light, and the sudden compression increases the temperature of the inner core to up to 100 billion kelvins.

Under this model, scientists believe that the distinctive plateau of the Type II-P supernovae is caused by the expulsion of most of the hydrogen envelope of the star. During the explosion, the shock wave ionizes the hydrogen in the outer envelope, which strips the electron from the hydrogen atom and results in a significant increase in the opacity. This prevents photons inside the envelope from escaping and causes the period of unvaried magnitude. When the hydrogen cools sufficiently to recombine, the outer layer becomes transparent and the light curve decreases again [8].

1.3 Experimental Devises

This observational experiment is made possible by the Las Cumbres Observatory global telescope network. The observations in this paper are based on the SBIG STL-6303 instrument with 0.4 meter telescope. The scientific imaging instrument contains Charge-coupled Device (CCD) which enables the camera to transform visual information into digital images. The instrument has readout noise of 14.5 electrons, a gain of 1.6 electron per ADU and a dark current of 0.03 electron per pixel per second. For the purpose of this experiment, filters SDSS i', SDSS r', SDSS g' are used [6]. SDSS i' has a wavelength center of 7545 Åand width 1290 Å. SDSS r' has a wavelength center of 6215 Åand width 1390 Å. SDSS g' has a wavelength center of 4770 Åand width 1500 Å.

The photometric analysis is based on Astroart 8, a software for astronomical image processing. We use Star Atlas, a mode of Astroart, to display star positions and to perform the astrometric or photometric calibration of a single image. To fix the reference stars, we identified those stars with GAIA DR3 star catalog created using the results obtained by Gaia space telescope.

2 Experimental Methods

2.1 Observational Design

AT2023hpb is a supernova discovered on May 1, 2023 at R.A. = 00h51m11s.790, Decl. = -73°11'30".30 with a magnitude of 14.2. Earlier report shows that its progenitor is a cataclysmic variable star [9]. We decided to observe this supernova because it has an appropriate magnitude for observation and analysis. As suggested by the professor and TAs, we requested two exposures for each of filters SDSS i', SDSS r', and SDSS g', each with integration time 100 seconds. We set the observational window to be every two days and repeated observations for two weeks. On May 20, 2023, we received the observational results which cover May 10, 11, 13, 14, 15, 16, 17, 18, 19, and 20. This results have a smaller range than what we requested. It turns out the images on May 20 are not usable, so we finally have data from the remaining nine days. Not all images are taken at the same observational sites.

2.2 Photometric Analysis

We use Astroart 8 for photometric analysis. The goal is to draw the apparent magnitude of the supernova at different filter on each day. Since two exposures are available at each filter on each day, we use the preprocessing mode to automatically align them and average the two images, which can reduce the noise and obtain a good signal-to-noise ratio (SNR).

We then pick the reference stars for photometry. We select four bright stars from the image as our reference stars, as shown in Fig 2. The information for the reference stars are shown in Fig 3.

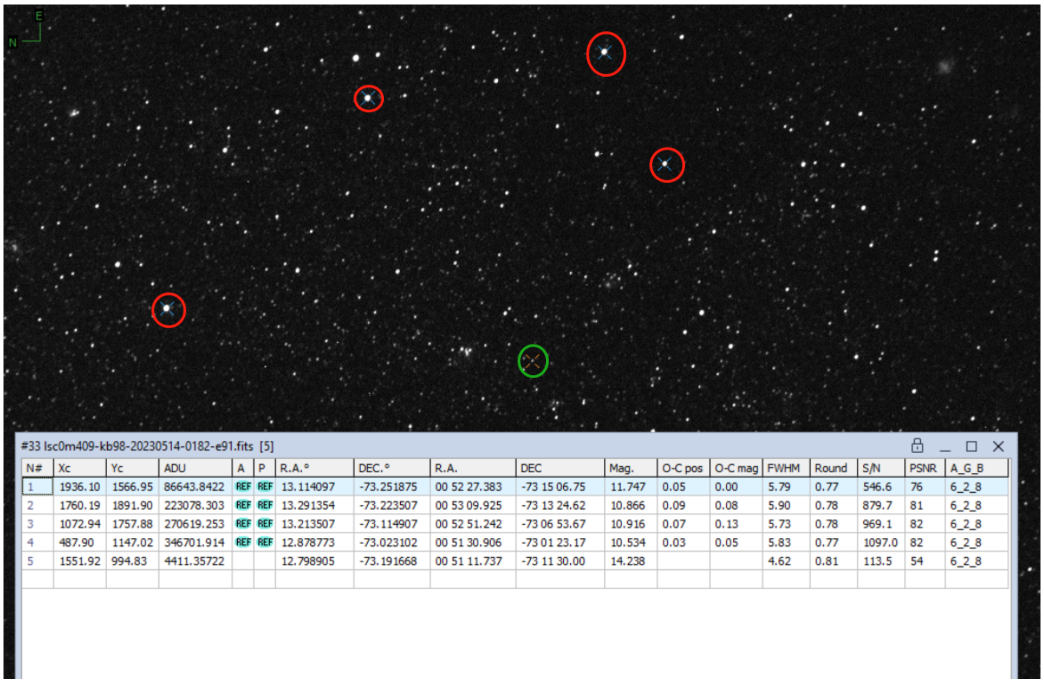

Figure 2: Operation process on Astroart. Stars in red circles are reference stars. The star in green circle is the objective supernova.

After picking the reference stars, we open Star Atlas and click "Reference stars, manual". The reference stars are then indicated on the star catalog (4). Once we click the same star on the catalog, its data including position and magnitude will be copied to the windows, set as reference stars, and ready for photometry.

Finally, we click astronotry and photometry and select the objective supernova based on its position. Its data will be calculated based on the ref-

Reference Stars	R.A.	DEC
1	00 52 51.242	-73 06 53.67
2	00 51 30.906	-73 01 23.17
3	00 53 09.925	-73 13 24.62
4	00 52 27.383	-73 15 06.75
Targeted Star	**R.A.**	**DEC**
AT2023hpb	00 51 11.790	-73 11 30.30

Figure 3: Information for the reference stars, as recorded in Google Sheet

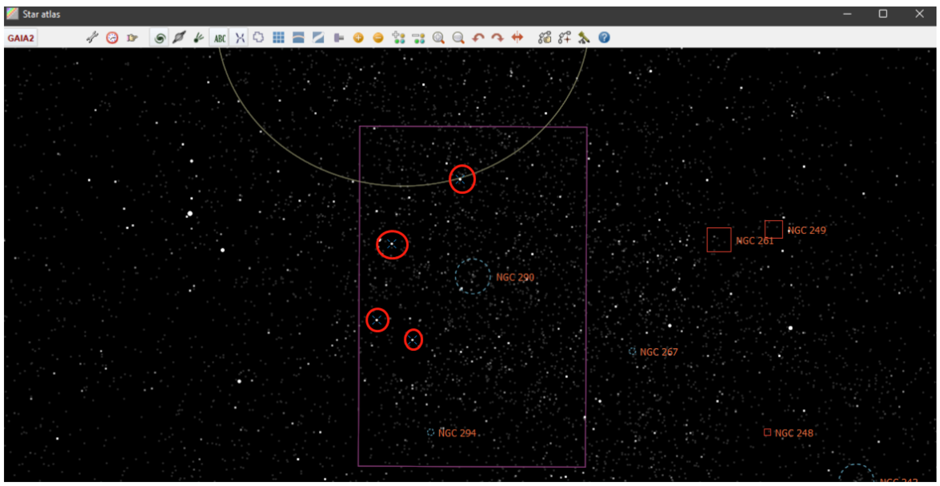

Figure 4: Selecting reference stars (indicated in red circles) on the Star Atlas

erence stars and shown in the windows. We record those data in Google Sheet.

We then repeat the whole procedure for each filter on each date. All the data is recorded in Fig. 5. We build light curves for each filter using python, as shown in Fig. 6, Fig. 7, and Fig. 8. We then reverse the y-axis of each graph to show the pattern of brightness and build a quadratic model to demonstrate the light curve using python, as shown in Fig. 9, Fig. 10, and Fig. 11.

2.3 Error Calculation

The main uncertainty propagated through the observational experiment is given by the signal-to-noise ratio (SNR). The higher the SNR, the better the quality of the image. The factors that determine SNR are related to the instrumental properties of the CCD camera. In principle, SNR in each measurement can be calculated manually with Equation 1 [1].

$$SNR = \frac{S}{N} = \frac{N_*}{\sqrt{N_* + n_{pix}(1 + \frac{n_{pix}}{n_B})(N_S + N_D + N_R^2 + G^2\sigma_f^2)}} \qquad (1)$$

In this equation, N_* is the total number of photons collected from the object of interest. n_{pix} is the number of pixels used in the integration of the signal from the object of interest. n_B is the total number of background pixels used to estimate the mean background level. N_S is the total number of photons per pixel from the background. N_D is the total number of the dark current electrons per pixel. N_R is the total number of electrons per pixel from readout noise. G is the gain of the CCD camera and σ_f is an estimate of the 1-sigma error. Those values can be found under each image as well as on SBIG STL-6303 website.

Luckily, the photometric system in Astroart has already calculated the SNR for each image, so we don't need to calculate it manually. To convert SNR into the uncertainty of apparent magnitude, we need to use Equation 2 [1].

$$\sigma_m = \frac{2.5}{ln(10) \cdot SNR} \tag{2}$$

3 Raw Data

Filter	Date (Site)	Magnitude	FWHM	Round	S/N	PNSR
SDSS i'	May 10 (LSC)	14.257	3.81	0.89	200.4	67
	May 11 (LSC)	14.377	3.66	0.91	188.5	65
	May 13 (LSC)	14.389	4.06	0.99	206.3	67
	May 14 (LSC)	14.38	4.30	0.81	193.3	64
	May 15 (LSC)	14.493	4.94	0.90	185.1	65
	May 16 (LSC)	14.584	4.39	0.93	192.8	66
	May 17 (COJ)	14.901	3.40	0.94	270.1	71
	May 18 (LSC)	14.585	4.25	0.91	197.0	66
	May 19 (COJ)	14.395	6.12	0.86	170.8	65
SDSS g'	May 10 (LSC)	14.026	4.77	0.52	99.1	53
	May 11 (LSC)	14.190	5.85	0.52	86.9	51
	May 13 (LSC)	14.284	4.90	0.82	113.8	53
	May 14 (LSC)	14.151	4.23	0.83	134.1	57
	May 15 (LSC)	14.238	4.62	0.81	113.5	54
	May 16 (LSC)	14.214	4.31	0.85	141.4	57
	May 17 (COJ)	14.229	3.55	0.82	201.5	62
	May 18 (LSC)	14.238	3.90	0.81	146.9	57
	May 19 (COJ)	13.609	6.79	0.92	139.1	57
SDSS r'	May 10 (LSC)	14.430	4.07	0.95	242.6	64
	May 11 (LSC)	14.507	3.61	0.88	223.5	63
	May 13 (LSC)	14.549	4.26	0.91	246.5	65
	May 14 (LSC)	14.449	4.38	0.90	249.0	65
	May 15 (LSC)	14.547	5.10	0.88	223.2	64
	May 16 (LSC)	14.666	4.55	0.87	243.7	65
	May 17 (LSC)	15.083	3.36	0.97	351.0	71
	May 18 (COJ)	14.735	4.13	0.84	244.9	65
	May 19 (COJ)	14.267	5.94	0.71	218.8	63

Figure 5: All the data of the objective supernova, as recorded in Google Sheet

In Fig. 5, FWHM is Full Width at Half Maximum, which is a measure of star size. Round is the ratio of Minor axis and Major axis of the FWHM (so it's 1.0 for a perfect round star). S/N is the signal-to-noise ratio (SNR). PNSR is a newly defined metric which can directly measure the noise on the image. Not all data in Fig. 5 is useful in the experiment.

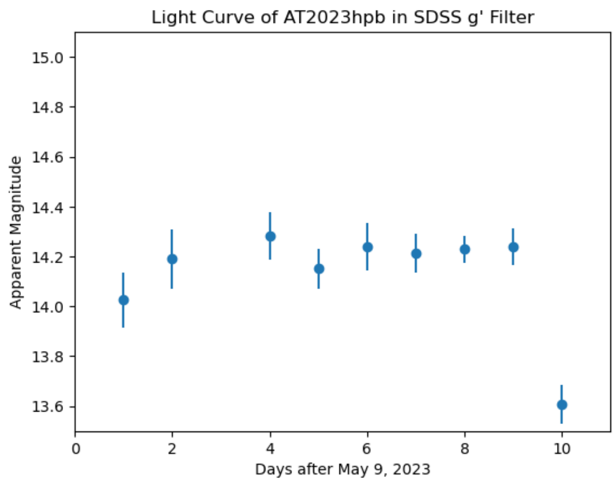

Figure 6: Light Curve of AT2023hpb in SDSS g' Filter

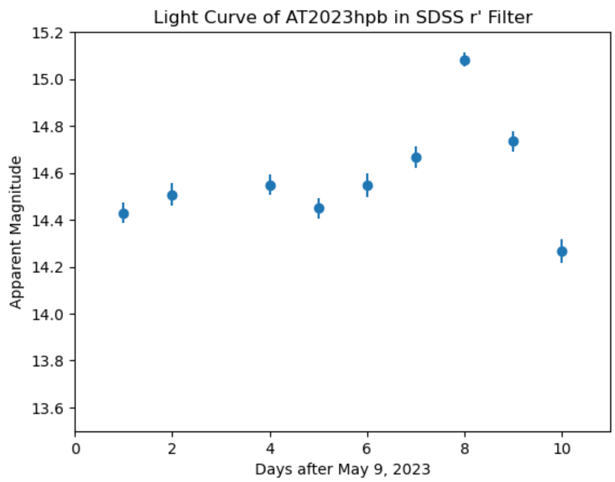

Figure 7: Light Curve of AT2023hpb in SDSS r’ Filter

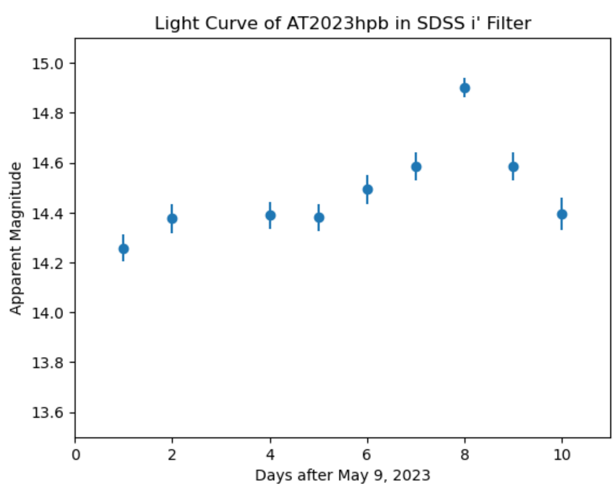

Figure 8: Light Curve of AT2023hpb in SDSS i’ Filter

4 Results

Some observations can be made from the light curves in different filters. First, all light curves demonstrate a general pattern that the luminosity of

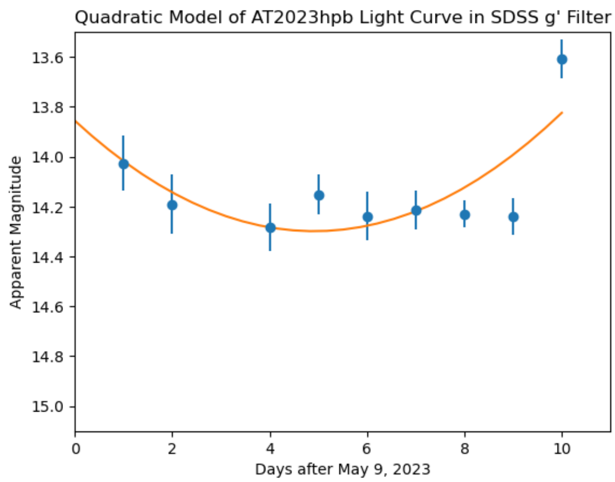

Figure 9: Quadratic Model of AT2023hpb Light Curve in SDSS g' Filter

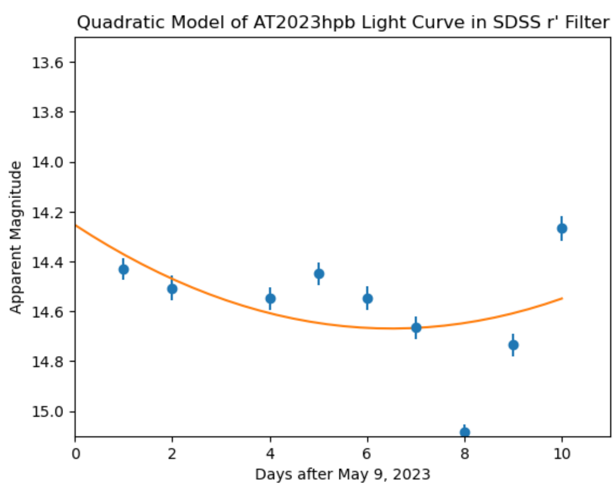

Figure 10: Quadratic Model of AT2023hpb Light Curve in SDSS r' Filter

the supernova is not strictly decreasing throughout the ten days. Rather, it gradually decreases in the first eight days and then increases to the original level before decreasing. In SDSS g' and SDSS r' filters, the objective supernova even becomes brighter at the tenth day than at the first day after

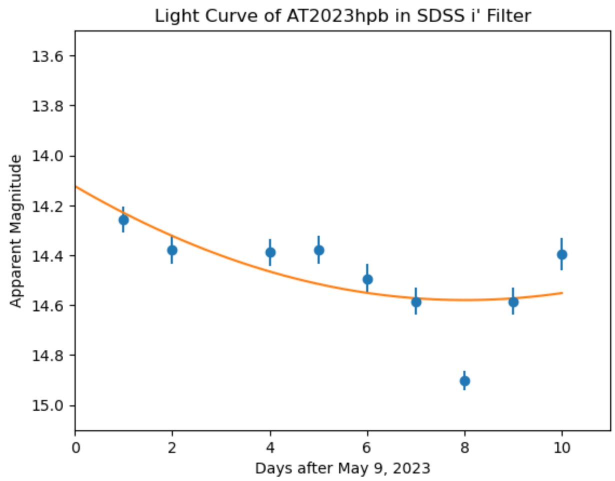

Figure 11: Quadratic Model of AT2023hpb Light Curve in SDSS i' Filter

May 9, 2023. Second, the light curves in SDSS i' and SDSS r' filters demonstrate a very similar pattern, while the supernova illuminates more light in the frequency range covered by the SDSS i' filter. This causes that the light curve in SDSS i' filter is 0.2 magnitude lower than that in SDSS r' filter. Third, the apparent magnitude in SDSS g' filter is much lower than that in other two filters on each date, especially after the eighth day of observation. This shows that the supernova illuminates more light in the frequency range covered by the SDSS g' filter, especially after the eighth day.

Scientists usually record the light curves of a given supernova for one or two month to decide its type. Our observations only record the light curves of the supernova for nine days one week after the date of discovery. However, given the light curves that we have constructed, we have good evidence that this supernova should be classified as Type II.

First, researches on theoretical light curves of Type II supernova have shown that its decay rate of apparent magnitude is much smaller than Type Ia supernova and usually becomes smaller after explosion. This is because The decay rate of the light curve depends on the isotopic decay rate happened in the Type II supernova at each period [5] [11]. The energy of the supernovae is emitted in two periods of radioactive decay: $^{56}Ni \rightarrow^{56} Co$ and $^{56}Co \rightarrow^{56} Fe$. Calculations show that in the first period the decay rate is 0.11 mag/day and in the second period 0.009 mag/day. The decay rate in the second period fits into the constructed light curves. Roughly, the light curves decline with a rate around 0.02 mag/day in SDSS r' filter in SDSS i' filter. In the SDSS g' filter, the magnitude even doesn't change throughout the ten days.

Second, the light curves that we have constructed don't fit into the theoretical light curves of Type Ia supernova. Researches have shown that the B band and V band light curves of Type Ia supernova demonstrate a rapid decline in brightness after explosion with the speed of 0.087 mag/day. The R band and I band light curves, however, demonstrates a "shoulder" or even a secondary maximum appearing about 20 days after maximum light in most cases [7]. This shows that the B band, I band, and R band light curves should have different patterns, as shown in Fig. 12. However, although the light curves in SDSS i' and SDSS r' do demonstrate a secondary maximum, the light curves in SDSS g' which have a frequency domain corresponding to B band and V band also demonstrate a increase in brightness, which, according to the theoretical light curves of Type Ia supernovae, should not occur. Thus, the objective supernovae cannot be classified as Type Ia.

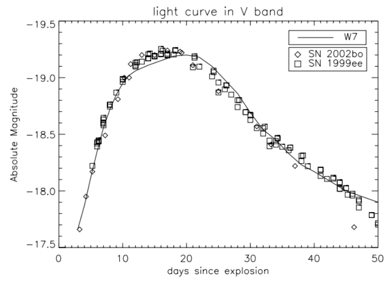

Fig. 12. LTE model light curve of the W7 explosion model in the *V* band compared to two observed SN Ia light curves of SN 1999ee and SN 2002bo.

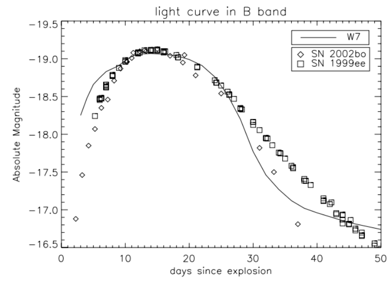

Fig. 14. LTE light curves of the W7 explosion model. The *B* band model light curve is too bright during the first few days.

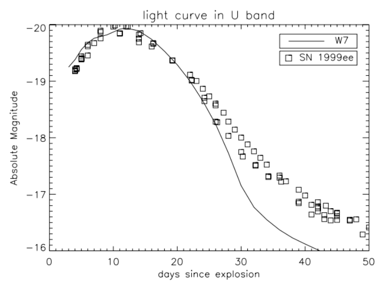

Fig. 13. *U* band light curve of the LTE model light curve compared to SN 1999ee.

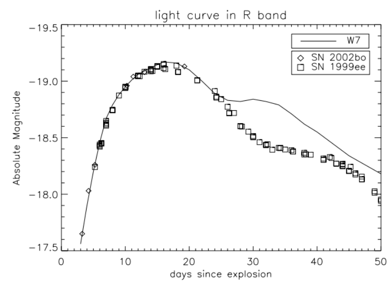

Fig. 15. The theoretical light curve in the *R* band seems to rise after a first decline after the maximum phase.

Figure 12: Theoretical Light Curves for Type Ia Supernovae [4]. A rapid decline of brightness is shown in U, B, and V bands.

5 Discussion

Although this observational experiment is more qualitative than quantitative, there are several ways that we can reduce the error and make our results more accurate. First, it turns out that the usual time span for the supernovae observations is one or two months. For Type II supernovae, the time span is even longer since its brightness changes much more slowly than that of Type Ia supernovae. Therefore, it is hard to draw any firm conclusion from the data we have received since a short range of data is more sensitive to error. Although we have good evidence to show that the objective supernova should be classified as Type II, more data is still necessary to support this conclusion. Of course, if we could do spectroscopy, then we can verify whether our analysis is correct. What's more, if we could have more data, we can further classify this supernova and distinguish whether it is Type II-P, Type II-L, or Type IIb.

References

[1] Philip J Castro, Tamara E Payne, Victoria C Frey, Kimberly K Kinateder, and Trenton J Godar. Calculating photometric uncertainty. In *Proceedings of the AMOS Technical Conference*, 2020.

[2] J. B. Doggett and D. Branch. A comparative study of supernova light curves. , 90:2303–2311, November 1985.

[3] Gerry Gilmore. The short spectacular life of a superstar. *Science*, 304(5679):1915–1916, 2004.

[4] D Jack, PH Hauschildt, and E Baron. Theoretical light curves of type ia supernovae. *Astronomy & Astrophysics*, 528:A141, 2011.

[5] K Nomoto, T Suzuki, T Shigeyama, S Kumagai, H Yamaoka, and H Saio. A type iib model for supernova 1993j. *Nature*, 364(6437):507–509, 1993.

[6] Las Cumbres Observatory. Filters. Accessed on June 12, 2023.

[7] Swinburne University of Technology. Type ia supernova light curves, 2007. Accessed on June 12, 2023.

[8] Swinburne University of Technology. Type ii supernova light curves, 2007. Accessed on June 12, 2023.

[9] Physics Purdue University, College of Science and Astronomy. Latest supernovae. Accessed on June 12, 2023.

[10] Massimo Turatto. Classification of supernovae. *Lect. Notes Phys.*, 598:21, 2003.

[11] Timothy R. Young. A Parameter Study of Type II Supernova Light Curves Using 6 M_{solar} He Cores. , 617(2):1233–1250, December 2004.